Journal of Cranio-Maxillo-Facial Surgery 47 (2019) 1054–1059

Contents lists available at ScienceDirect

Journal of Cranio-Maxillo-Facial Surgery

journal homepage: www.jcmfs.com

Virtual reconstruction of bilateral midfacial defects by using statistical shape modeling

Marc Anton Fuessinger [a, *], Steffen Schwarz [a], Joerg Neubauer [b], Carl-Peter Cornelius [c], Mathieu Gass [a], Philipp Poxleitner [a], Ruediger Zimmerer [d], Marc Christian Metzger [a], Stefan Schlager [a]

[a] Department of Oral and Maxillofacial Surgery (Chairman: Prof. Dr. Dr. Rainer Schmelzeisen), Albert-Ludwigs University Freiburg, Hugstetterstr. 55, 79106, Freiburg, Germany
[b] Department of Radiology (Chairman: Prof. Dr. Fabian Bamberg), Albert-Ludwigs University Freiburg, Hugstetterstr. 55, 79106, Freiburg, Germany
[c] Department of Oral and Maxillofacial Surgery (Chairmann: Prof. Dr. Dr. Michael Ehrenfeld), Ludwig-Maximilians University Munich, Lindwurmstr. 2a, 80137, Munich, Germany
[d] Department of Oral and Maxillofacial Surgery (Chairmann: Prof. Dr. Dr. Nils Claudius Gellrich), Medical School Hanover, Carl-Neuberg-Straße 1, 30625, Hannover, Germany

ARTICLE INFO

Article history:
Paper received 9 December 2018
Accepted 25 March 2019
Available online 1 April 2019

Keywords:
Statistical shape model (SSM)
Computer-assisted surgery (CAS)
Virtual defect reconstruction
3D planning
Virtual planning

ABSTRACT

Purpose: Mirroring and manual adaptation as the main virtual reconstruction method of midfacial defects is time demanding and ignores asymmetrical skull shapes. By using a statistical shape model (SSM), the reconstruction can be automatized and specified. The current study aims to show the ability of the SSM in the virtual reconstruction of artificial bilateral defects.
Methods: Based on 131 pathologically unaffected CT scans of the adult midface region, an SSM was created. DICOM data were generated, segmented and registered on one mesh, which serves as template for the SSM. The SSM consists of the registered surface meshes and includes the shape variability of the cranial vault. Fractured or missing parts were calculated by the known shape variability of healthy midface data. Using 25 CT scans not included in the SSM, the precision of the reconstruction of virtually placed bilateral defects of the orbital floor (Group 1) and bilateral naso-orbital-ethmoid (NOE) fractures (Group 2). Distances to the corresponding parts of the intact skull were calculated to show the accuracy of the virtual reconstruction method.
Results: All defects could be reconstructed by using the SSM and GM technique. The analysis shows a high accuracy of the SSM-driven reconstruction, with a mean error of 0.75 ± 0.18 mm in group 1 and with a mean error of 0.81 ± 0.23 mm in group 2.
Conclusion: The precision of the SSM-driven reconstruction is high and its application is easy for the clinician because of the automatization of the virtual reconstruction process in the field of computer-assisted surgery (CAS). Respecting of the natural asymmetry of the skull and the methods of GM are reasons for the high precision and the automatization of the new shown reconstruction workflow.

1. Introduction

The precise manual repositioning of bone fragments and the adaptation of individually bent osteosynthesis plates with their anatomical repositioning are critical steps during surgical intervention. Especially the orbital cavity with its thin bone structures and the reduced intraoperative visibility is sensitive to volumetric changes and bone steps (Frohwitter et al., 2018). Imprecision in fragment repositioning and an enlarged orbital cavity cause functional problems like diplopia and eye movement limitations (Bittermann et al., 2014; Frohwitter et al., 2018; Schonegg et al., 2018).

The fine repositioning of bone fragments is crucial and can be ensured by the use of the well-known computer-assisted surgery (CAS) and its helpful tools, like navigation and patient-specific

* Corresponding author.
E-mail addresses: marc.anton.fuessinger@uniklinik-freiburg.de (M.A. Fuessinger), steffen.schwarz@uniklinik-freiburg.de (S. Schwarz), joerg.neubauer@uniklinik-freiburg.de (J. Neubauer), peter.cornelius@med.lmu.de (C.-P. Cornelius), mathieu.gass@uniklinik-freiburg.de (M. Gass), zimmerer.ruediger@mh-hannover.de (R. Zimmerer), marc.metzger@uniklinik-freiburg.de (M.C. Metzger), stefan.schlager@anthropologie.uni-freiburg.de (S. Schlager).

https://doi.org/10.1016/j.jcms.2019.03.027
1010-5182/

implants (PSI) (Dreizin et al., 2018; Jansen et al., 2018; Scolozzi, 2017). CAS consists of the key elements of (i) analysis of the defect, (ii) planning the reconstruction by using tools like mirroring and registration, (iii) virtual surgery to reposition the bone fragments, and (iv) generating surface meshes for intraoperative navigation or production purposes for PSI. As a planning tool, the mirroring method is still the most applied technique (Dreizin et al., 2018; Metzger et al., 2006). Based on the assumption of a symmetrical facial anatomy, an unaffected region is mirrored on a symmetrical plane to reconstruct missing or comminuted bone areas. Manual adaptation and alignment of the mirrored area must be done to gain a smooth transition to the surrounding uninjured anatomical regions (Bell et al., 2009; Fuessinger et al., 2017b). The obtained surface can be exported to produce a fracture model as bending template for osteosynthesis plates or as a landmark for intraoperative navigation or as a template for manufacturing PSIs(Dreizin et al., 2018). The time-consuming step has to be done preoperatively at the desk of the surgeon, thus reducing the routine clinical application. Clinicians demand an automated and easy-to-handle tool without too much required hardware capacity because of a lack of financial support from the government. Moreover, the known procedures are limited to unilateral defects. For bilateral defects or comminuted fractures of the midface, manual repositioning of the dislocated bone fragments must be performed with regard to the unaffected anatomic landmarks of the affected side (Metzger et al., 2007).

Our proposed statistical shape model (SSM)-driven reconstruction method is based on diffeomorphic deformations and principal component analysis (PCA) to extract the main modes of variation. The suggested workflow needs segmented CT data and at least four landmarks, which are placed on prominent anatomical positions. The registration of the SSM on the defect midface serves as a tool to find the model instance most suitably matching the anatomical structure of the unaffected parts of the target skull.

To evaluate our SSM-driven approach, 14 midfaces with artificial uni- and bilateral defects of the orbital floor and medial wall were virtually reconstructed. Evaluation was done calculating the distance to the original surface of the unaffected area and by comparison to the mirroring method as the gold standard.

We aim to automatize the reconstruction process for orbital floor fractures and complex bilateral NOE-fractures to overcome limitations and “shortcomings” of known planning tools in the CAS workflow, like mirroring and registration. Improvements in the CAS workflow must be suitable for clinical application, with the main focus on reduction of the on-screen time for the surgeon and on better usage of the 3D radiological data, i.e. cone beam CT and CT.

2. Material and methods

The method consists of the combination of geometric morphometrics (GM) and a data-driven reconstruction of midface defects based on an SSM. For valid reconstruction, an SSM implements empirical knowledge for reconstructing the cranial shape by including a high variability of healthy samples. In this study, the region of interest (ROI) was set on the midfacial region. Open-source software packages for the statistical/mathematical platform R were used for statistical analysis. According to the best-practice rules for R packages, the applied software will be cited.

2.1. Defect creation

To define the same defect in all patients’ CT scans, we created the defects on a skull template not included in the SSM. The vertex indices of the coordinates within the defect regions were recorded. The template was then subsequently matched to the segmented specimens using a diffeomorphic registration procedure provided by the R-package ANTsR (Avants et al., 2015). As a result, the mesh representation of the surface shares its mesh topology with all the registered specimens and removal of the indexed vertices from the registered meshes results in similar defects being created throughout the sample.

The defects on the template were created as follows: The segmented skull was imported in the 3D modeling software Blender. (Blender Foundation, Amsterdam, The Netherlands) (Hess, 2007). “UV spheres” were created, modified and symmetrically placed within the orbital floor and the NOE region. For the orbital floor defects a typical fracture pattern with sparing the palatinal bone is simulated (Fig. 1).

By adding a procedural operation, the spheres were subtracted from the midfacial skull.

The defect creation of the NOE complex is done similarly. One individually designed sphere is placed in the area of the NOE (Fig. 2). The same procedural operation is used to substract the sphere from the template.

2.2. Statistical shape model fitting

The presented new method requires a manual and an automated part. The patient's CT scan is segmented by a simple gray-value thresholding technique to get a surface mesh. On the surface mesh, presenting the effect midface, four landmarks are placed. The anatomical positions of the landmarks are the nasion, the fronto-zygomatical suture, and the ledge of the palatinal bone. The landmarks establish an initial spatial correspondence between the target shape and the SSM, which also constrains the SSM to shapes with similar landmark positions.

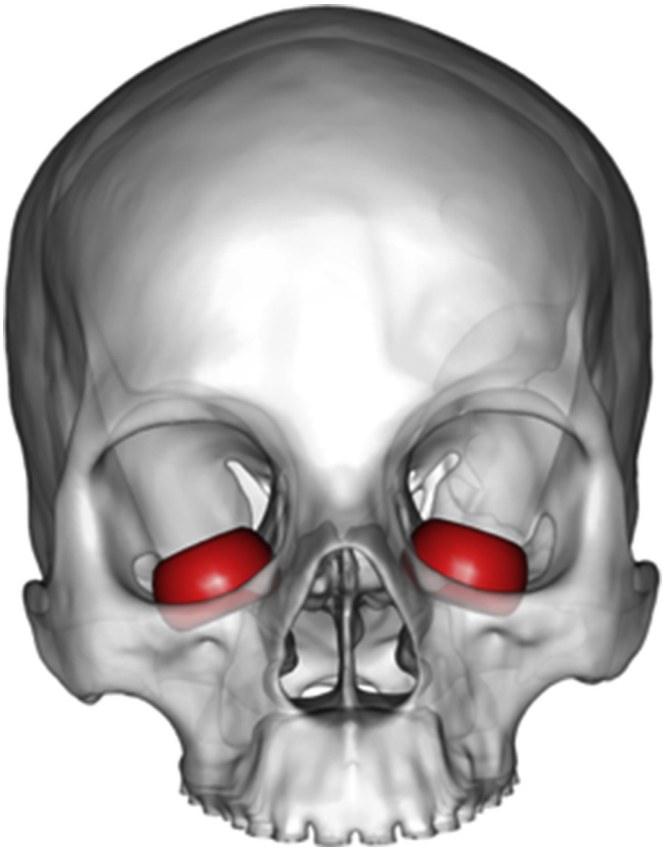

Fig. 1. Adding spheres (red) symmetrically in the area of the orbital floor of the skull template for standardized resection.

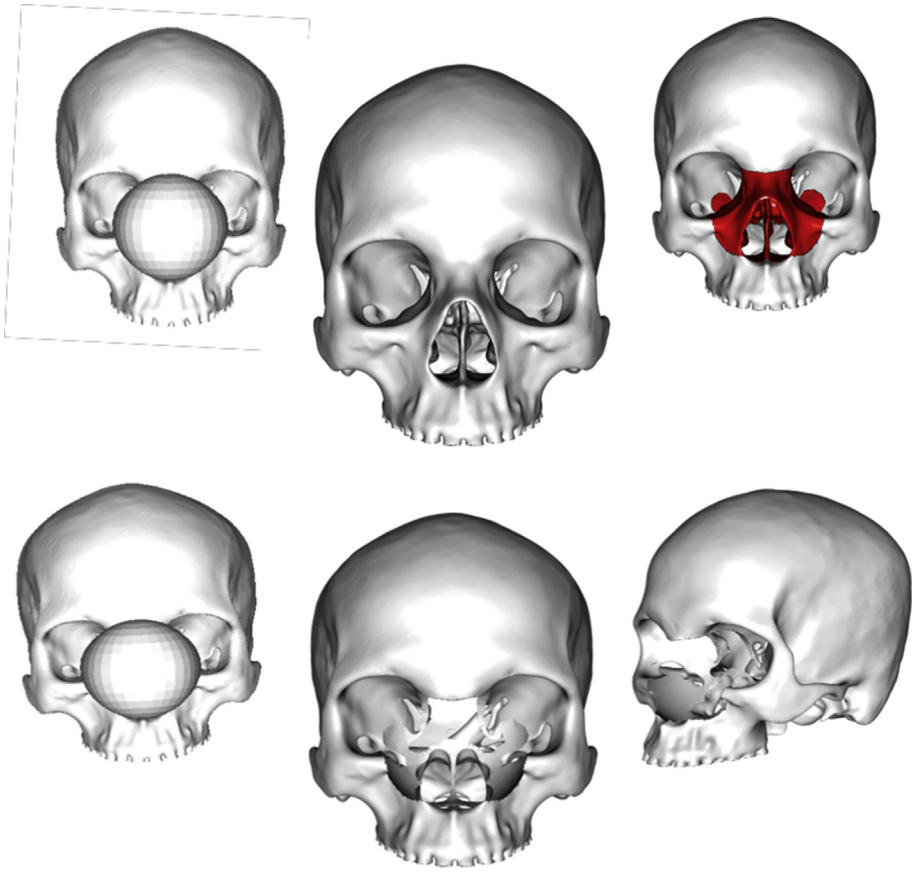

Fig. 2. Adding one sphere (red) in the area of the NOE complex on the skull template for standardized resection.

From now on, the automatized workflow begins. The mean shape from the SSM is adapted to the target surface. A precise alignment is done by the rigid iterative closest point (ICP) technique. To get a posterior SSM, the original SSM is constrained on the corresponding counterparts of the target midface. Containing shapes only in the vicinity of the landmarks, the posterior SSM is placed on the target mesh to allow isotropic variation around the landmark position with a standard deviation (SD) of 2 mm. The mean of the posterior SSM serves as a starting point to search appropriate instances to minimize the symmetric distance to the target skull. For this step, an elastic ICP, based on smoothed displacement fields, is performed. The result is an SSM instance that is very similar to the target shape. The target surface is mostly a close match, but not an exact one, because it is not included in the shape variability of the SSM.

2.3. Error evaluation

For evaluating the prediction error, we chose the following metrics for both types of defects:

- Mean error = the average error within the ROI for each patient
- Max. error = the maximum error within the ROI for each patient
- Percentage of Vertices below a given error threshold: here, we evaluated this error metric for 1, 1.5 and 2 mm.

Using the fact that all specimens are registered to the same template, these errors were computed by assessing the distance between the vertices within the defect region to the surface of the predicted skulls. This allows generation of error statistics for each vertex within the ROIs, as these are (pseudo-)homologous throughout the testing sample.

3. Results

The error distributions for mean and max. error are shown in Figs. 3 and 4. The mean error for the NOE cases is 0.81 mm (SD = 0.23) and 0.75 mm for the Bioccular case (SD = 0.18).

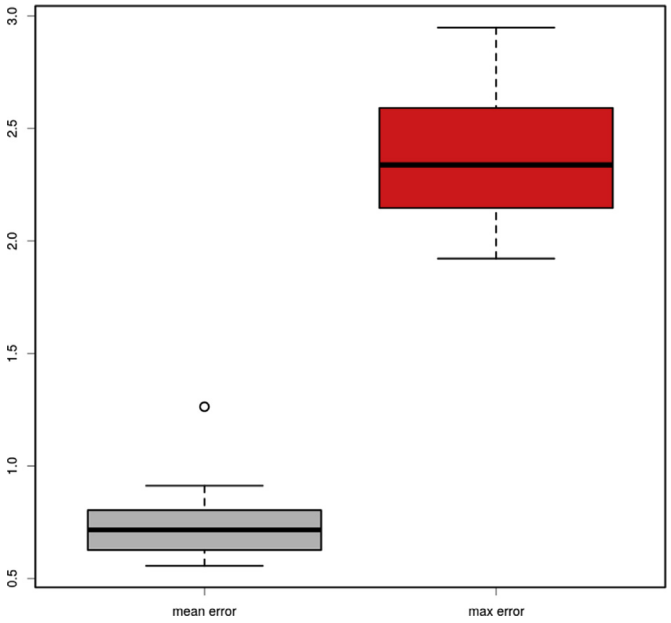

Fig. 3. Boxplots visualizing the reconstruction error distribution of the Bioccular case.

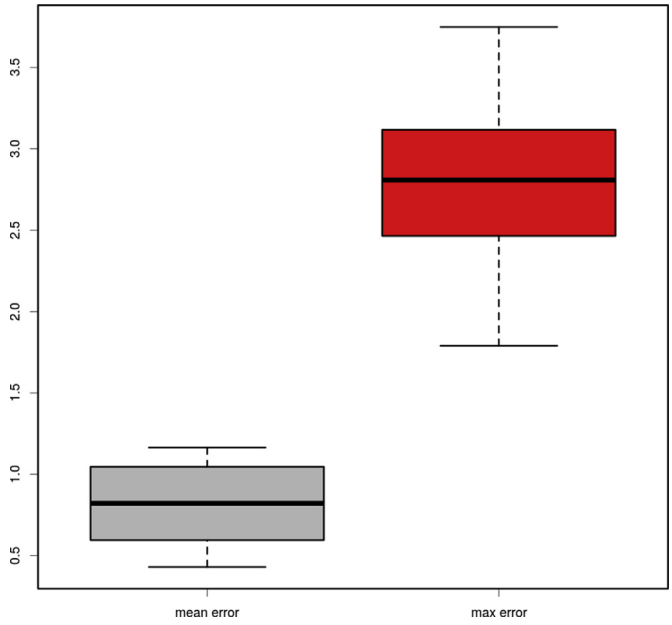

Fig. 4. Boxplots visualizing the reconstruction error distribution of the NOE case.

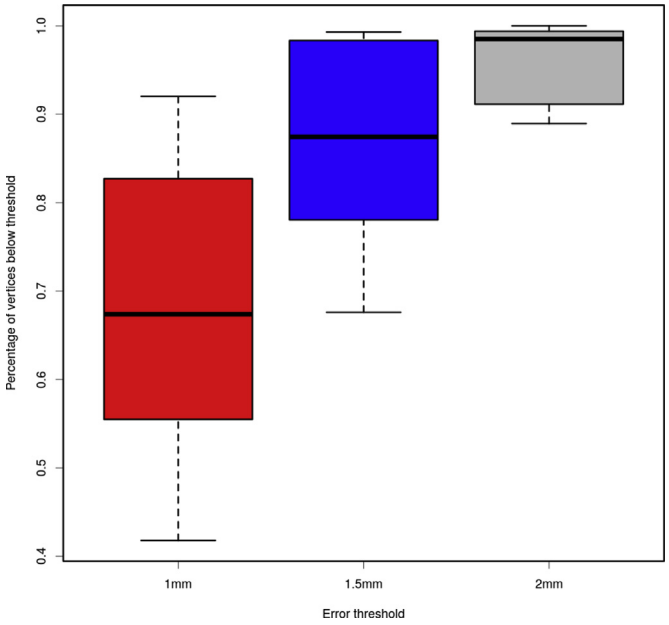

Fig. 6. Boxplot visualizing the percentage of vertices below a given threshold of the NOE defects.

The maximum errors are 2.8 mm for the NOE case (SD = 0.57) and 2.37 mm for the Bioccular case (SD = 0.36) (Figs. 3 and 4).

Regarding the amount of vertices below a given error threshold (Figs. 5 and 6), it can be shown that Prediction accuracy is higher in the intraorbital defects: In all but one patient more than 80% of the vertices are predicted with an error below 1.5 mm. However, regarding the NOE defects this amount decreases, very likely due to the fact that a much larger coherent region is to be predicted. Here, a much wider range of errors can be seen and only at a threshold of 2 mm 90% of vertices are below this error margin.

Figs. 7 and 8 show heat maps visualizing the per-vertex average errors.

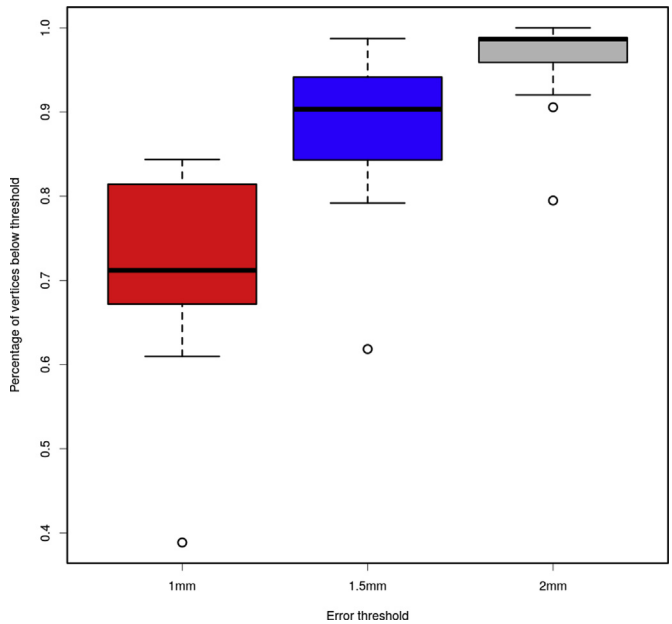

Fig. 5. Boxplot visualizing the percentage of vertices below a given threshold of the Bioccular defects.

4. Discussion

Automatized virtual reconstruction of midfacial defects is essential for the further success of CAS. The benefits of virtual planning, such as enhanced precision and time saved intra-operatively, will be accessible for a wide range of patients world-wide if the planning step is simplified (Dawirs et al., 2017; Zimmerer et al., 2017). The described pathway of a modified SSM is not just an extended database suitable to find a corresponding

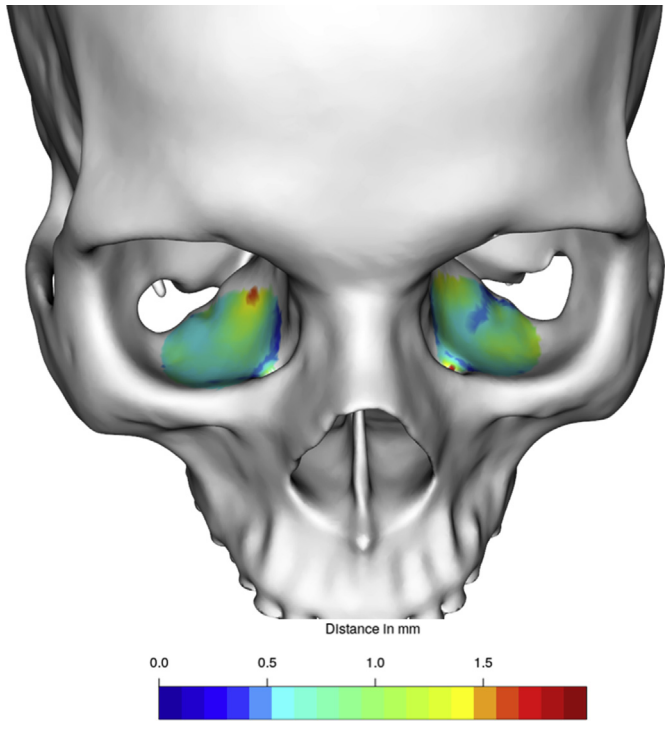

Fig. 7. Heat maps visualizing the per-vertex average errors of the Bioccular defects calculating in the area of the orbital floor with parts of the medial wall.

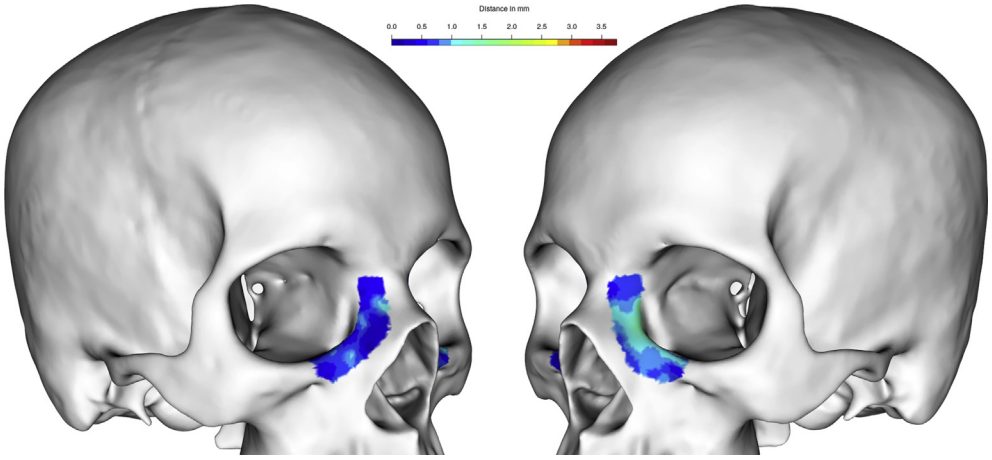

Fig. 8. Heat maps visualizing the per-vertex average errors of the NOE defects calculating in the area of the medial orbital wall.

template for the individual patient skull. It is an independent computer algorithm that searches fitting vertices out of a point cloud which in itself is part of a Gaussian distribution. Despite the self-learning computer algorithm, the database used relies on CT scans of a Caucasian population. For a worldwide application of the proposed SSM workflow, regional CT scans must be added to guarantee the described high precision.

In contrast to the known procedure of mirroring with manual steps like defining the mirroring plain and the manual alignment of the mirrored objects on the defect area, the SSM reduces the need for manual interaction to a minimum. Except for defining four landmarks, which can be placed with a tolerance of about 1 mm, the reconstruction is done automatically. If there is a conflict of a fracture line to a landmark position, landmarks can be changed. The new position just has to be adjusted in the underlying dataset of the SSM.

As previously shown, the SSM workflow offers a higher precision in dealing with skull defects, compared to the mirroring procedure (Fuessinger et al., 2017a; Semper-Hogg et al., 2016).

On the one hand, the precision achieved by using the mirroring procedure for virtual reconstruction of unilateral defects seems to be high enough clinically (Dubois et al., 2015). On the other hand, taking into account that the generated precise surface serves as a basis for the manufacturing of PSIs, deviations from the original surface that are generated in the virtual reconstruction process will be added to the imprecision of the known workflow of imaging, segmentation and production of PSIs and will lead to clinically relevant discrepancies. This is true especially if the workflow is simplified and accelerated by enhancing the reconstructive precision.

Besides the increased precision, the proposed workflow simplifies and accelerates the preoperative planning steps and guarantees an enhanced preoperative reconstructive quality. The corresponding computer algorithm will be available as an Internet platform, on which the surgeon uploads the CT dataset and receives a reconstructed surface to continue the adaption of PSIs or a stereolithographic file for 3D printing.

5. Conclusion

The presented approach is a highly efficient method for the reconstruction of bilateral midface defects. The surgeon benefits from an automated reconstruction algorithm and the patients receive a very precise reconstruction, highly similar to the original situation. The shown SSM can easily be integrated in clinical reconstruction software packages and will be evaluated in clinical situations in complex midfacial fractures.

Ethical approval

All procedures performed in studies involving human participants were in accordance with the ethical standards of the institutional and/or national research committee and with the 1964 Helsinki declaration and its later amendments or comparable ethical standards.

Disclosure of potential conflicts of interest

The authors declare that they have no conflict of interest.

Compliance with ethical standards

Institutional ethics committee approval (450/15) by University Freiburg, Germany. All applicable international, national, and/or institutional guidelines for the care and use of animals were followed.

Research involving human participants and/or animals

This article does not contain any studies with human participants or animals performed by any of the authors. For this type of study formal consent is not required.

Authors agreements to the submission

All authors have viewed and agreed to the submission.

Informed consent

This article does not contain patient data.

Funding

There was no funding of this study. This research did not receive any specific grant from funding agencies in the public, commercial or non-profit sector.

Appendix A. Supplementary data

Supplementary data to this article can be found online at https://doi.org/10.1016/j.jcms.2019.03.027.

References

Avants BB, Kandel BM, Duda JT, Cook PA, Tustison NJ, Shrinidhi KL: ANTsR: ANTs in R; 2015

Bell RB, Markiewicz MR: Computer-assisted planning, stereolithographic modeling, and intraoperative navigation for complex orbital reconstruction: a descriptive study in a preliminary cohort. J Oral Maxillofac Surg 67: 2559–2570, 2009

Bittermann G, Metzger MC, Schlager S, Lagrèze WA, Gross N, Cornelius C-P, et al: Orbital reconstruction: prefabricated implants, data transfer, and revision surgery. Fac Plast Surg FPS 30: 554–560, 2014

Dawirs K, Haßfeld S: Virtuelle Welt in der Mund-, Kiefer- und Gesichtschirurgie. Der MKG Chirurg 10: 231–233, 2017

Dreizin D, Nam AJ, Hirsch J, Bernstein MP: New and emerging patient-centered CT imaging and image-guided treatment paradigms for maxillofacial trauma. Emerg Radiol 25(5): 533–545, 2018

Dubois L, Jansen J, Schreurs R, Saeed P, Beenen L, Maal TJJ, et al: Predictability in orbital reconstruction: a human cadaver study. Part I: endoscopic-assisted orbital reconstruction. J Craniomaxillofac Surg Offic Publ Eur Assoc Craniomaxillofac Surg 43: 2034–2041, 2015

Frohwitter G, Wimmer S, Goetz C, Weitz J, Ulbig M, Kortuem KU, et al: Evaluation of a computed-tomography-based assessment scheme in treatment decision-making for isolated orbital floor fractures. J Craniomaxillofac Surg 46: 1550–1554, 2018

Fuessinger M, Semper-Hogg W, Bittermann G, Schmelzeisen R, Metzger M: Innovationen in der DysgnathiechirurgieModern concepts in orthognathic surgery. Der MKG Chirurg 10: 263–271, 2017a

Fuessinger MA, Schwarz S, Cornelius CP, Metzger MC, Ellis 3rd E, Probst F, et al: Planning of skull reconstruction based on a statistical shape model combined with geometric morphometrics. Int J Comput Assist Radiol Surg 4: 519–529, 2017b

Hess R: The essential Blender: guide to 3D creation with the open source suite blender. No Starch Press, 2007

Jansen J, Schreurs R, Dubois L, Maal TJJ, Gooris PJJ, Becking AG: The advantages of advanced computer-assisted diagnostics and three-dimensional preoperative planning on implant position in orbital reconstruction. J Craniomaxillofac Surg 46: 715–721, 2018

Metzger MC, Hohlweg-Majert B, Schön R, Teschner M, Gellrich N-C, Schmelzeisen R, et al: Verification of clinical precision after computer-aided reconstruction in craniomaxillofacial surgery. Oral Surg Oral Med Oral Pathol Oral Radiol Endodont 104: e1–e10, 2007

Metzger MC, Schön R, Schulze D, Carvalho C, Gutwald R, Schmelzeisen R: Individual preformed titanium meshes for orbital fractures. Oral Surg Oral Med Oral Pathol Oral Radiol Endodont 102: 442–447, 2006

Schonegg D, Wagner M, Schumann P, Essig H, Seifert B, Rucker M, et al: Correlation between increased orbital volume and enophthalmos and diplopia in patients with fractures of the orbital floor or the medial orbital wall. J Craniomaxillofac Surg 46: 1544–1549, 2018

Scolozzi P: Applications of 3D orbital computer-assisted surgery (CAS). J Stomatol Oral Maxillofac Surg 118: 217–223, 2017

Semper-Hogg W, Fuessinger MA, Schwarz S, Ellis E, Cornelius C-P, Probst F, et al: Virtual reconstruction of midface defects using statistical shape models. J Craniomaxillofac Surg Offic Publ Eur Assoc Craniomaxillofac Surg 45: 461–466, 2016

Zimmerer RM, Dittmann J, Gellrich N-C: Virtuelle techniken in der Traumatologie. Der MKG Chirurg 10: 252–262, 2017